

Simulation-driven formulation of transportation fuel surrogates

Krithika Narayanaswamy ^{a*} and Perrine Pepiot ^{b**}

^aDepartment of Mechanical Engineering, Indian Institute of Technology Madras, Chennai, India;

^bSibley School of Mechanical and Aerospace Engineering, Cornell University, New York, NY, USA

(Received 7 July 2016; accepted 1 April 2018)

An alternative way to formulate transportation fuel surrogates using model predictions of gas-phase combustion targets is explored and compared to conventional approaches. Given a selection of individual fuel components, a multi-component chemical mechanism describing their oxidation kinetics, and a database of experimental measurements for key combustion quantities such as ignition delay times and laminar burning velocities, the optimal fractional amount of each fuel is determined as the one yielding the smallest error between experiments and model predictions. Using a previously studied three-component jet fuel surrogate containing *n*-dodecane, methyl-cyclohexane, and *m*-xylene as a case study, this article investigates in a systematic manner how the surrogate composition affects model predictions for ignition delay time and laminar burning velocities over a wide range of temperature, pressure and stoichiometry conditions, and compares the results to existing surrogate formulation techniques, providing new insights on how to define surrogates for simulation purposes. Finally, an optimisation algorithm is described to accelerate the identification of optimal surrogate compositions in this context.

Keywords: Surrogate definition; chemical kinetics; ignition delay times; laminar flame speeds; jet fuel

1. Introduction

Incorporating chemical kinetics in computational studies of combustion systems is necessary to understand the combustion characteristics of transportation fuels, address the problem of combustion control, predict emissions, and optimise engine performance. However, the inherent complexity of those fuels prevents the direct use of detailed chemical models, and requires the introduction of a simplified fuel representation. Typically, transportation fuels are modelled using a representative surrogate mixture, i.e. a well-defined mixture comprised of a few components chosen to mimic the desired physical and chemical properties of the real fuel under consideration.

For simplicity of exposition, we choose to focus here on gas-phase surrogates for kerosene, or jet fuel. Yet all methods referenced or developed below are equally applicable to all fuel types with appropriate, but straightforward changes. Most earlier studies (for instance, [1–6]) defined surrogate compositions by matching the average amount of the major chemical classes: alkanes, cyclo-alkanes, and aromatics, with typical distribution for jet fuel being 79%, 10%, and 11% by mole, respectively [7,8]. Following the recommendations of Violi et al. [4] and Colket et al. [9], the procedure to formulate surrogate compositions

*Corresponding author. Email: krithika@iitm.ac.in

**Email: perrine.pepiot@cornell.edu

was subsequently refined (e.g. [10–13]) to additionally reproduce target properties such as hydrogen-to-carbon (H/C) ratio, density, cetane number, threshold sooting index (TSI), and average molecular mass between the surrogate and the jet fuel.

Later, Dooley et al. [12–14] put forth the idea of not including every chemical class present in the real fuel within the surrogate, but rather only those necessary to form intermediate species of markedly different potential for radical production and consumption. They obtained their surrogate by matching the aforementioned combustion targets, except that they considered derived cetane number over the conventional cetane number. The real fuel as well as the surrogate mixture were investigated experimentally in several configurations (such as flow reactors, ignition delays, flame speeds, and extinction limits) and found to show similar extents of chemical reactivities. Further, Won et al. [15] experimentally found that surrogates matching the ratio of methyl to methylene functional groups, in addition to these global targets, reproduce the low temperature kinetic phenomena as well. Their studies also showed that upon matching combustion property targets, the actual molecular compositions of the real fuel could be emulated by the surrogate [13], suggesting that knowing the average chemical structure of the real fuel, appropriate surrogate fuels can be proposed. Yu et al. [16] advanced such a functional group based approach recently. Through these studies, the global property targets have been demonstrated as a reliable measure of the combustion behaviour investigated in these studies for the real fuels.

Despite knowing the experimentally formulated surrogate compositions for kerosene fuels from the works of Dooley et al. [12–14], many other surrogate mixtures are considered in practice, motivated by the availability of compact kinetic models to integrate with computational studies and their accuracy. Besides other approaches [4,13,17], given a set of components to make up a surrogate, its composition can be determined using a constrained optimisation algorithm, as was done for example in [11], and more recently in [18]. Surrogate fuel properties are estimated from the individual components using either simple mole or mass fraction-weighted mixing rules (e.g. H/C ratio) or more complex quantitative structure/property relationships (e.g. cetane number or TSI, see for example [19]). The percentage amount of each component is then optimised in order to match as closely as possible the chosen set of target properties of an average real fuel (e.g. [18]). One must note that depending on the choice of the number and nature of the surrogate components, it may not be mathematically possible to match one or all real fuel properties exactly, in which case choices have to be made on the relative importance of the selected target properties in the optimisation process.

The procedure outlined above to determine the surrogate composition relies entirely on the assumption that a clear correlation exists between the fuel composition and the property of interest that can conveniently be expressed in the form of a mixing rule weighted by the mass or mole fraction of each component. Depending on the property, such a mixing rule can reflect a conserved quantity (e.g. atomic composition) or be derived from empirical observations, which introduces a significant degree of uncertainty in the formulas used (e.g. cetane number and TSI). In the best case, even if those errors are minimal and an appropriate surrogate mixture is arrived at, in the context of combustion simulations, it is not entirely guaranteed that such a surrogate is the best to represent the real fuel, since uncertainties and model choices that affect the computations significantly have not been accounted for while defining the surrogate.

This is particularly well acknowledged when considering the reaction mechanisms used in the simulations – kinetic models of even comprehensively studied fuel components (typically chosen to constitute surrogates) show some deficiencies and predict different combustion behaviours. Therefore, a given surrogate composition may yield quite different

results when employed in combustion simulations depending on the chosen kinetic model. The objective of the present work is to investigate if this coupling between the surrogate fuel and the associated kinetic model can be explicitly established at the surrogate fuel formulation stage itself.

Broadly, the goal is to investigate the following: (i) in the context of combustion simulations, given a complex fuel to model and a set of fuel components, is the conventionally determined surrogate composition already the one with the best predictive capabilities, or can better predictions be obtained with a different composition? (ii) If yes, how different would such a composition be from the conventional one? A direct comparison of these two options, based on choice of the underlying kinetic model, is the focus of the present article. Thus, this work serves as a first step to bring in the characteristics and predictive capabilities of the chemical kinetic mechanism used for the simulations within the surrogate formulation framework.

To be specific, we explore and analyse a different strategy to define surrogates, in which model predictions for simple zero and one-dimension configurations over a wide range of conditions are used to identify an optimal surrogate composition. We begin by introducing some notations and a graphical framework in Section 2 in order to simplify the analyses to follow, and use this framework to provide some perspectives on existing procedures to define surrogate compositions, taking the work of Narayanaswamy et al. [18] on a *n*-dodecane, methyl-cyclohexane, *m*-xylene jet fuel surrogate as reference case. In Section 3, we analyse for a given kinetic mechanism how the surrogate composition affects the prediction of experimentally measured jet fuel ignition delay times and laminar flame speeds, and identify the composition that best reproduces those experimental measurements. Section 4 describes a nonlinear optimisation algorithm to quickly evaluate the optimal surrogate composition identified in Section 3, and conclusions are provided in Section 5.

2. Notations and graphical representation

We consider a three-component surrogate mixture containing *n*-dodecane (NC12), methyl-cyclohexane (MCH), and *m*-xylene (XYL). We denote by X_{NC12} , X_{MCH} , and X_{XYL} their respective mole fractions in the multi-component surrogate mixture. These satisfy the constraints:

$$0 \leq X_{\text{NC12}}, X_{\text{MCH}}, X_{\text{XYL}} \leq 1 \quad (1)$$

$$X_{\text{NC12}} + X_{\text{MCH}} + X_{\text{XYL}} = 1. \quad (2)$$

For ease of analysis, the set of all possible mixtures of *n*-dodecane, methylcyclohexane, and *m*-xylene can be represented in the form of a triangle, as shown in Figure 1.

The edges of the triangle serve as axes for the mole fractions of each of the three components, varying from 0 to 1. A point located at a vertex corresponds to a pure component. Each point inside the triangle corresponds to a different mixture, whose composition can be obtained by successively projecting it onto each of the three component axes, along a direction parallel to the edge opposite to the $X = 1$ vertex associated with this component. For example, in Figure 1, since $X_{\text{MCH}} = 1$ is found at the top of the triangle, the methyl-cyclohexane mole fraction of a given mixture is obtained by projecting *horizontally* onto the MCH axis. Discretising each edge with N points ($N = 11$ in Figure 1), we obtain a total

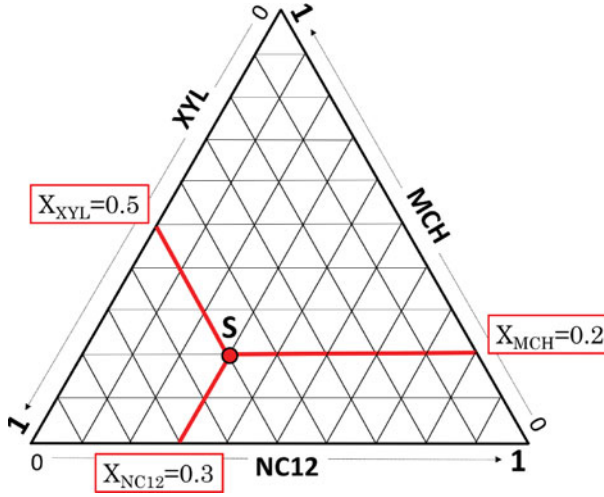


Figure 1. Graphical representation of all possible compositions of a three-component (*n*-dodecane, *m*-xylene, and methyl-cyclohexane) jet fuel surrogate. Inner mesh illustrates how the resulting composition space is discretised using increments of $\Delta X = 0.1$ ($N=11$ grid points on each side), and how to relate a point *S* inside the triangle to its actual composition.

of:

$$N_G = \frac{1}{2}N(N+1) \quad (3)$$

surrogate compositions uniformly distributed within the triangle. This discretisation and triangular representation is used throughout the rest of the manuscript to visualise the performance of different surrogate compositions.

One such informative visualisation can be done by considering the constrained optimisation approach followed in [18]. In this work, the surrogate composition was determined by matching as closely as possible (1) the H/C ratio, (2) the cetane number (CN), and (3) the TSI of an average jet fuel. Jet fuel specifications only provide ranges for those quantities, and typical values based on several sources in the literature [20–25] are:

$$\begin{aligned} \text{H/C} &= 1.91 \pm 0.05, \\ 42 &\leq \text{CN} \leq 47, \text{ and} \\ 14 &\leq \text{TSI} \leq 26. \end{aligned} \quad (4)$$

The regions over which each individual constraint is satisfied are shown in Figure 2. To determine cetane numbers for mixtures of components, in the absence of a more accurate relationship that describes the interactions between the neat molecules chosen in the surrogate and their mixtures, a linear volume fraction weighted mixing rule is used here [26,27], although this can be less accurate [28,29] because of the nonlinear interactions between the fuel molecules. Figure 2 demonstrates graphically that there exists a range of compositions for which all constraints are satisfied. By construction, the optimal surrogate determined in Narayanaswamy et al. [18] and denoted by \mathcal{S}_o belongs to the overlapping region, with a composition of 30.3% *n*-dodecane, 48.5% methyl-cyclohexane, and 21.2% *m*-xylene (by mole%).

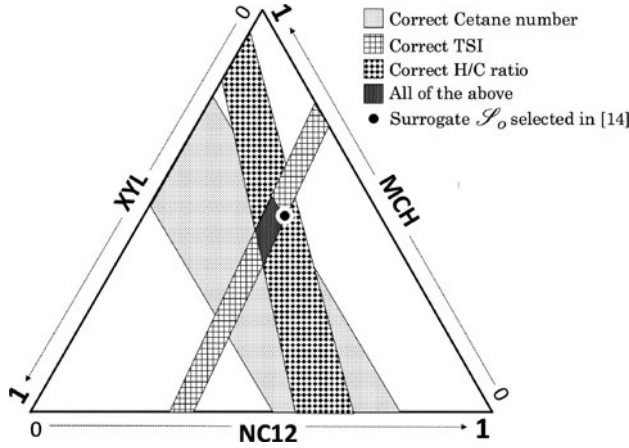


Figure 2. Surrogate compositions satisfying the constraints on cetane number (grey), threshold sooting index (squares), or H/C ratio (black diamonds) as defined in Equation (4). Compositions satisfying all of them simultaneously are shown in dark, while the surrogate \mathcal{S}_o proposed in Narayanaswamy et al. [18] is indicated by a solid black circle.

The surrogate \mathcal{S}_o , coupled with the compact multi-component kinetic mechanism also developed in [18], was shown to satisfactorily reproduce experimental measurements over a wide range of configurations and conditions. We now propose to quantify and analyse how the agreement with experimental data could be improved if, instead of using these global target properties to define the surrogate composition, *the experimental data themselves are used as targets*. This is detailed in the next section.

3. Simulation-driven surrogate compositions

3.1. Problem set-up

The following experimental data are chosen as targets:

- (1) Ignition delays [30] at $\phi = 1.0$, pressures ranging from 8 atm to 39 atm, and temperatures ranging from 700 K to 1400 K;
- (2) Laminar flame speeds [31] at $P = 1$ atm, $T_u = 403$ K, and equivalence ratios $0.7 \leq \phi \leq 1.4$.

The surrogate composition space is uniformly discretised using 33 grid points on each edge, for a total of 561 possible mixtures. For each of these mixtures, ignition delays at all experimental conditions are computed using the multi-component chemical kinetic mechanism derived in Narayanaswamy et al. [18] using a component library approach applied on a series of consistent single-component mechanisms [32–34]. Calculating flame speeds at several equivalence ratios for such a large number of mixtures is computationally expensive. Instead, pure component flame speeds are computed over the desired range of conditions, and are used to estimate the mixtures flame velocities using a previously validated correlation rule (described in section 4.4.2 of Ref. [18]):

$$\ln \text{SL}^{\text{mix}} = \sum_{i=1}^3 \left\{ X_i N_i \frac{T_{ad}^i}{T_{ad}^{\text{mix}}} \ln \text{SL}^i \right\}, \quad (5)$$

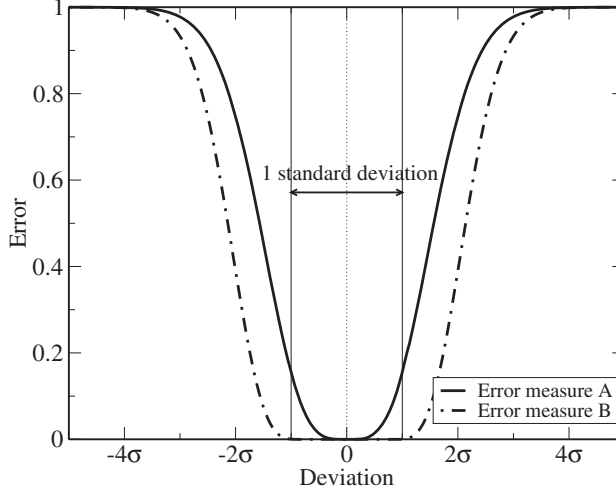


Figure 3. Model prediction errors used to evaluate the error functions $F_{\text{ig}}^{\text{mix}}$ and $F_{\text{SL}}^{\text{mix}}$ as a function of the actual deviation between the model prediction and the experimental measurement. Standard deviations are taken as 25% for all ignition delay cases, and $\pm 2 \text{ cm s}^{-1}$ for laminar burning velocities.

where

$$T_{ad}^{\text{mix}} = \frac{\sum_{i=1}^3 X_i N_i T_{ad}^i}{\sum_{i=1}^3 X_i N_i}, \quad (6)$$

index $i = \{1, 2, 3\}$ corresponds to the fuel components: *n*-dodecane, methylcyclohexane, and *m*-xylene, respectively, X_i is the mole fraction of the i th component in the fuel mixture, N_i the total number of moles of products (obtained from the equilibrium composition), T_{ad}^i is the adiabatic flame temperature, and SL^i is the laminar flame speed of the pure component i . Equations (5) and (6) are evaluated for a fixed equivalence ratio ϕ , which in turn, is varied from lean to rich.

3.2. Error measure

The agreement between model predictions and experimental data for all feasible surrogate mixtures is measured using the error function F^{mix} , defined as

$$F^{\text{mix}} = \frac{1}{2} \left(F_{\text{ig}}^{\text{mix}} + F_{\text{SL}}^{\text{mix}} \right), \quad (7)$$

where $F_{\text{ig}}^{\text{mix}}$ and $F_{\text{SL}}^{\text{mix}}$ are calculated as the sum of the model prediction errors over all experimental conditions for the ignition cases and the laminar flame speed cases, respectively. To account for the uncertainty in the experimental measurements, a Gaussian function is adopted to evaluate individual errors, as illustrated in Figure 3. As a first choice, the error function labelled “A” in Figure 3 is used unless stated otherwise.

Accordingly, for a given surrogate mixture (denoted by “mix”), the error in ignition delay prediction is evaluated as:

$$F_{\text{ig}}^{\text{mix}} = \frac{1}{N_{\text{ig}}} \sum_{i=1}^{N_{\text{ig}}} \left\{ 1 - \exp \left(\frac{-(\tau_{\text{sim},i}^{\text{mix}} - \tau_{\text{exp},i})^2}{2\sigma_i^2} \right) \right\}^2 \quad (8)$$

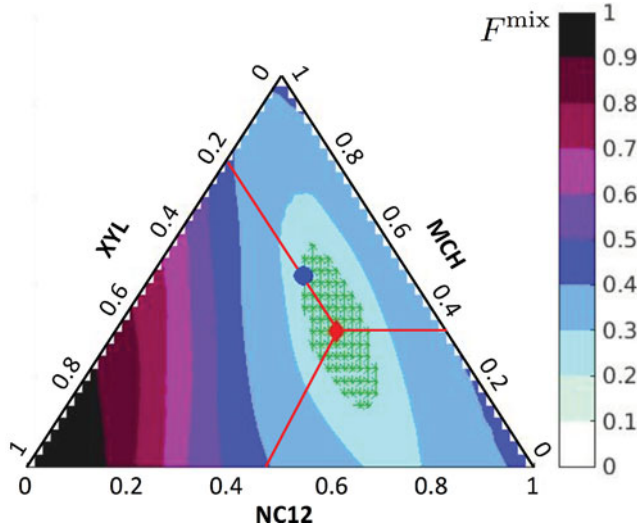


Figure 4. Error function F^{mix} evaluated throughout the surrogate composition space, highlighting \mathcal{S}_o (blue circle) and the newly defined simulation-based composition \mathcal{S}_s (red diamond). The region over which F^{mix} is less than 5% above its minimum value is highlighted with green symbols.

where N_{ig} is the number of ignition delay data points considered in the experimental dataset, and τ denotes the ignition delays with subscripts specifying experiments (exp) or simulations (sim). A constant standard deviation $\sigma = \pm 25\%$ of the mean value is used, which corresponds to the reported uncertainty in the experimental data of Wang and Oehlschlaeger [30]. Similarly for the laminar flame speeds, $F_{\text{SL}}^{\text{mix}}$ is given by:

$$F_{\text{SL}}^{\text{mix}} = \frac{1}{N_{\text{SL}}} \sum_{i=1}^{N_{\text{SL}}} \left\{ 1 - \exp \left(\frac{-(\text{SL}_{\text{sim},i}^{\text{mix}} - \text{SL}_{\text{exp},i})^2}{2\sigma_i^2} \right) \right\}^2 \quad (9)$$

where N_{SL} is the number of flame speed measurements, and SL denotes the laminar flame speed with subscripts specifying experiments (exp) or simulations (sim). A constant standard deviation $\sigma = \pm 2 \text{ cm s}^{-1}$ is used, which corresponds to the uncertainty reported in the experimental flame speed measurements of Hui et al. [31].

Note that the configuration-specific error functions $F_{\text{ig}}^{\text{mix}}$ and $F_{\text{SL}}^{\text{mix}}$, along with the combined one, F^{mix} , all yield values bounded between 0 and 1. Despite being normalised by the number of data points of each type, we acknowledge that the datasets for flame speeds are at atmospheric pressure, whereas ignition delays are at different pressures. A impartial weighting procedure that accounts for this difference in conditions will be examined in the future, while the focus here remains on elucidating the overall idea.

3.3. Performance map and optimal composition

The error function F^{mix} is computed over the entire surrogate composition space, as described above. The results are shown in Figure 4, with darker colors being associated with larger errors. Among all compositions tested, the one yielding the least error ($\sim 26\%$, red diamond) is made of 43.75% *n*-dodecane, 34.375% methyl-cyclohexane, and 21.875%

m-xylene by mole%. This composition as will henceforth be referred to as the simulation-based surrogate, or \mathcal{S}_s , to distinguish it from the composition \mathcal{S}_o introduced earlier.

3.4. Remarks and discussion

Several interesting remarks can be made from Figure 4.

- A. The mixtures on the left half of the triangle contain significant amounts of *m*-xylene at the expense of *n*-dodecane and methyl-cyclohexane. Those mixtures show large errors (>40%) compared to experimental data, and are therefore not suitable as surrogates for jet fuels.

This is expected from figure 6 in [18], which shows that the ignition delays of *m*-xylene are much longer compared to those of actual jet fuel at high temperatures. Also, *m*-xylene cannot describe the ignition behaviour at moderate and low temperatures exhibited by jet fuels.

- B. About 10% of all mixtures tested have relative errors of less than 5% (green symbols) from the optimal surrogate \mathcal{S}_e , and this set includes \mathcal{S}_o (blue circle).

To illustrate this, a comparison of ignition delays and flame speeds of \mathcal{S}_e and \mathcal{S}_o in Figure 5 shows the extent of similarity in predictions between these mixtures. The laminar flame speed predictions of these two mixtures are indistinguishable. For the ignition delay configurations, surrogate \mathcal{S}_s represents data at $P = 20$ atm better than \mathcal{S}_o at $T < 900$ K, while compromising on the few data points at those temperatures at $P = 11$ atm. The significant improvement with surrogate \mathcal{S}_s appears at low temperatures ($T < 750$ K) at $P = 20$ atm and this will be discussed subsequently. No conclusive remark can be made about predictions at $P = 39$ atm, since both surrogates show shorter ignition delays compared to experimental data at these conditions. Thus, while it is not possible to obtain a perfect agreement between model prediction and experimental measurements, both the surrogates can be regarded as similarly appropriate to represent the ignition delay data (at stoichiometric conditions, especially at $T > 750$ K) as well as flame speed data. Smaller uncertainties in the reference data (especially ignition delays) would reduce the size of the low-error region, likely increasing the differences between optimal and non-optimal mixtures.

- C. The low-error region, highlighted in green, has a significant overlap with the region satisfying the H/C ratio constraint (shown in Figure 2), but limited overlap with the region satisfying the cetane number constraint. In fact, in the low error region, the cetane numbers can vary from 46 to 62. Note that the optimal surrogate composition \mathcal{S}_s has a H/C ratio of 1.95, well within the expected range, but a cetane number of 56.15, therefore outside the range specified in Equation (4).

The optimal surrogates for different reference experimental datasets are shown in Figure 6.

It can be seen that the optimal surrogate which best reproduces ignition delays of jet fuel (Figure 6(a)) belongs to a different region of the triangular composition space than the one that best reproduces the flame speeds (Figure 6(b)). Thus, the surrogate that best represents both these datasets, i.e. \mathcal{S}_s (Figure 4), is a compromise between the two. The flame speed data used to calibrate the surrogate composition in effect tend to constrain the

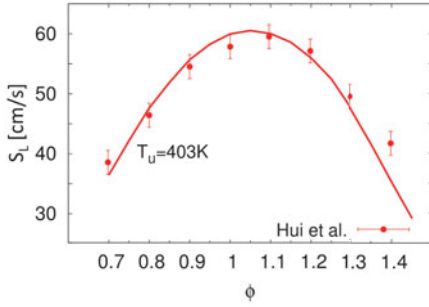
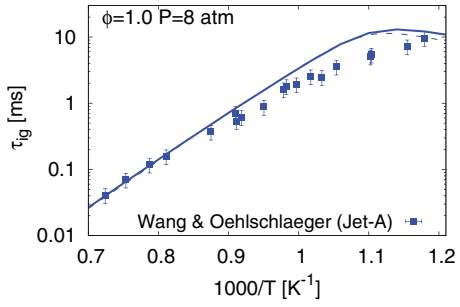
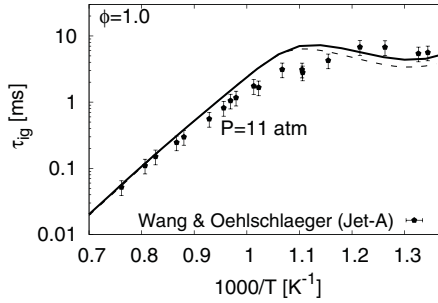
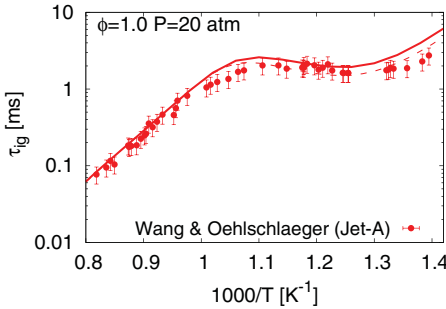
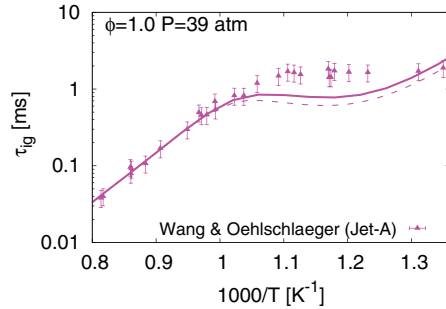
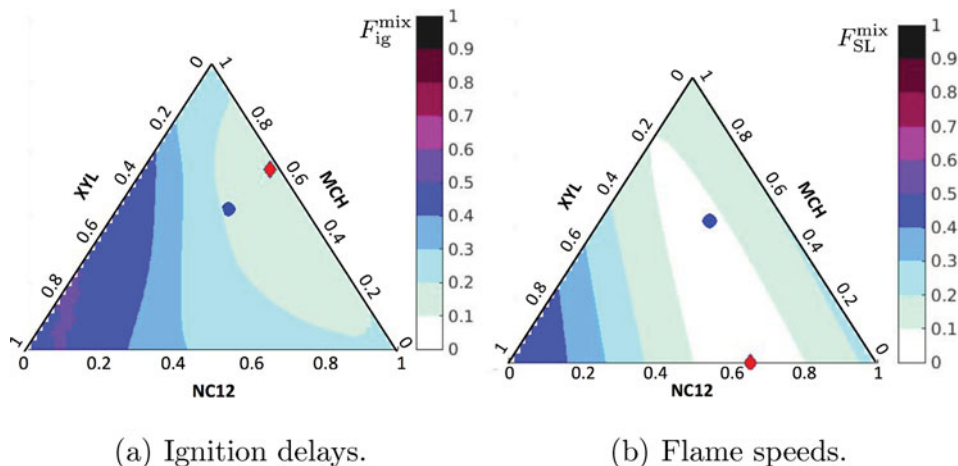

 (a) $P = 1 \text{ atm}, T_u = 403 \text{ K}$

 (b) $P = 8 \text{ atm}$

 (c) $P = 11 \text{ atm}$

 (d) $P = 20 \text{ atm}$

 (e) $P = 39 \text{ atm}$

Figure 5. (a) Computed laminar flame speeds at $P = 1 \text{ atm}$ and (b)–(e) ignition delays at stoichiometric conditions for (i) \mathcal{S}_o proposed in [18] based on the constrained optimisation approach (solid lines) and (ii) \mathcal{S}_s identified in Section 3.3 based on model predictions (dashed lines); experimental data (symbols) [30,31].

H/C ratio of the optimal surrogate to fall within the prescribed range for jet fuels (1.91 ± 0.05 [20,21]). This observation emphasises the need to correctly weigh the errors coming from different datasets or combustion configurations.

More interestingly, note that the ignition delays simulated with surrogate \mathcal{S}_o predicts longer low temperature ignition delays compared to experiments (see solid lines in



(a) Ignition delays.

(b) Flame speeds.

Figure 6. Error in predictions compared to experiments calculated as root mean square of $1 - \text{Gaussian deviation}$, with reference data as (a) ignition delays only, (b) laminar flame speeds only, (c) both ignition delays and laminar flame speeds (same as Figure 4). Surrogate \mathcal{S}_o is shown by a blue sphere. The best mixtures in cases (a), (b) and (c) are all indicated by red diamonds.

Figure 5(d) at $T < 750$ K). This difference, despite the cetane number of surrogate \mathcal{S}_o (equal to 46.6) falling within the typical range for jet fuel (42–47 [24,25]), may suggest a need to improve the kinetic mechanism proposed in [18] for low temperature ignition. It is therefore expected that when using this reaction mechanism to describe the kinetics, a surrogate designed to match the jet fuel cetane number (as done for \mathcal{S}_o) overpredicts ignition delays at low temperatures, because of the inaccuracies in the reaction mechanism at those conditions. The simulation-based \mathcal{S}_s automatically corrects for this behaviour, by choosing a mixture with a H/C ratio ($H/C = 1.95$) corresponding to that of the real fuel, thereby capturing S_L and high temperature ignition, but with a higher cetane number (56.15) than typical jet fuels (42–47 [24,25]). This allows for a better prediction at lower temperatures (Figure 5(d)). This suggests that *in a computational modelling context, surrogate compositions should be determined not just based on global characteristics, as has been done so far, but also on the characteristics and predictive capabilities of the chemical kinetic mechanisms used for the simulation.*

This is illustrated further in the Supplementary materials by considering jet fuel surrogates made of *n*-dodecane, toluene and methylcyclohexane. Different optimal surrogate compositions are identified based on the presented approach using the kinetic mechanism described above [18] and jetSurF [35], depending on the predictive capabilities of the respective kinetic model.

D. \mathcal{S}_s is found to lie outside of the range of TSIs specified for jet fuel.

With no experimental data representative of the sooting tendency, there is actually no reason why the TSI constraint would be satisfied. This point is illustrated in Figure 7, where the surrogates \mathcal{S}_o and \mathcal{S}_s are shown to predict significantly different amounts of polycyclic aromatic hydrocarbons in rich propagating flames. Therefore, it can be expected that the picture as shown in Figure 4 may change dramatically as additional experimental data, which characterise sooting or other combustion aspects, are included as reference

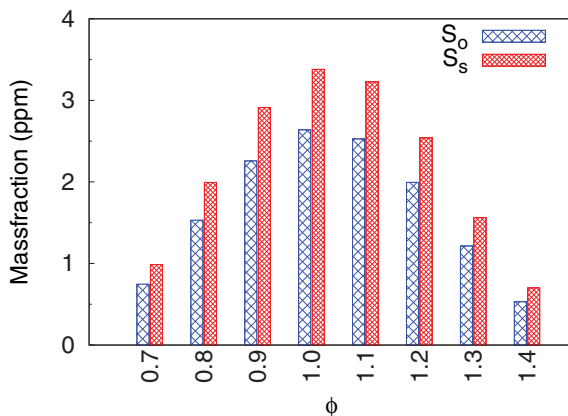


Figure 7. Maximum amount of polycyclic aromatic hydrocarbons (one ring to four rings) present in premixed flames, as predicted with surrogates \mathcal{S}_o and \mathcal{S}_s as initial fuels.

data. This, again, emphasises the importance of designing a surrogate specifically for the numerical simulations of interest.

E. The results indicate a weak sensitivity to the error measure employed.

To investigate the sensitivity of the optimal surrogate to the error measure used, we consider another error measure, labelled “B” in Figure 3, in place of the one used above to define the error function $F_{\text{ig}}^{\text{mix}}$ (Equation (8)) and $F_{\text{SL}}^{\text{mix}}$ (Equation (9)). Accordingly, all predictions that fall within the uncertainty limits of the reference experimental data are assigned a zero error, taking these as perfect in comparison to the mean value of data. Outside the uncertainty limits, the error between the computed results and the reference data grows as Gaussian deviations, approaching unity (or 100% error) for very large deviations. The rest of the procedure is unchanged. The resulting optimal mixture is 46.875%, 31.25%, and 21.875% for *n*-dodecane, methyl-cyclohexane, and *m*-xylene, respectively. This error of roughly 3% for the first two components corresponds to the grid spacing chosen to construct the performance map (33 points per edge): the optimal surrogate therefore moved one grid point away from \mathcal{S}_s . While this suggests a weak sensitivity for the optimal surrogate identified by the approach with respect to the error measure employed, this aspect must be revisited when more accurate reference data (especially ignition delays) become available.

The above discussion suggests that the approach to define surrogates based on actual experimental data of combustion characteristics is promising. Note that the manner in which the experiments are modelled may have inaccuracies (due to facility effects). In the presented approach, the uncertainties in the experimental data need to be carefully assigned to account for these differences and this aspect warrants further investigation.

4. Nonlinear optimisation procedure

The optimal simulation-based surrogate \mathcal{S}_s was identified above from the performance maps directly. While this brute force approach revealed a lot of information about the proposed surrogate formulation strategy, highlighting its strengths and scope for improvement, it is unnecessarily expensive, especially if the experimental dataset is large, or if more than three components are considered for the surrogate. Instead, only a few carefully

chosen mixtures need to be evaluated to find the error function minimum if an optimisation approach is followed, increasing greatly the practicality of the procedure. The details of this automatic nonlinear optimisation approach are given below.

The nonlinear optimisation library NLOpt, an open-source library for nonlinear optimisation available from Massachusetts Institute of Technology [36], is used in the present framework, and the FlameMaster code [37] is used to evaluate ignition delay times and laminar burning velocities. The variables to optimise are naturally chosen as the mole fractions of two out of three (or in general, of the number of components minus one) of the surrogate components, the last component amount being deduced from the mole fractions normalisation condition. As mentioned above, the most expensive part of the optimisation algorithm is the repeated evaluations of the error function F^{mix} for large chemical kinetic mechanisms and large experimental datasets. To accelerate the process significantly, we therefore adopt the sensitivity analysis-based method proposed by Davis et al. [38], in which response surfaces are constructed in the vicinity of the point under consideration in the optimisation algorithm. As expected, with a small enough convergence criterion for the optimisation algorithm, the resulting surrogate composition is located less than one grid point away from \mathcal{S}_s , containing 42.8% *n*-dodecane, 36.5% methylcyclohexane, and 20.6% *m*-xylene by mole%.

Note that the correlation rule, Equation (5), is used here as well to determine the laminar flame speeds of mixtures in order to compare the surrogates in the two approaches in a fair manner. Since the optimisation approach involves far fewer computations compared to the brute force method, laminar flame speeds could now be computed easily for the desired mixtures and the response surface can be created for S_L based on these calculations.

A Fortran version of the code used to perform this optimisation can be obtained from the authors upon request. This code can handle any chemical kinetic mechanisms, and can easily be extended to account for more than three surrogate components, different error functions, and other simulation configurations and combustion targets of interest.

5. Conclusions

In this article, an alternate approach to define surrogates for gas-phase combustion applications based on model predictions of an experimental dataset has been analysed, and its strengths have been highlighted using a previously well-characterised jet fuel surrogate. In contrast to the global combustion characteristics (such as hydrogen-to-carbon ratio, cetane number, etc.) used as targets in existing surrogate definition approaches, the proposed method places the focus on (i) the predictions of combustion dynamics such as ignition delay times or laminar flame speeds and their agreement with experimental data, and (ii) the characteristics of the kinetic mechanism used to obtain those predictions.

This is a very important distinction: while a surrogate may *a priori* satisfies all specifications for the fuel of interest, if the corresponding chemical mechanism is not able to capture the fundamental combustion quantities at the core of the turbulent combustion models used in the simulations, one cannot expect to obtain reasonable predictions in those simulations either. Thus, in a computational modelling context, surrogate compositions *should be determined not just based on global characteristics, as has been done so far, but also on the characteristics and predictive capabilities of the chemical kinetic mechanisms used for the simulation.*

The nonlinear optimisation code to formulate surrogate compositions based on model prediction is available from the authors. This flexible code can be extended to handle

any surrogate mixture of interest, and can become, in the authors' opinion, a valuable contribution to the combustion community.

Acknowledgements

The authors thank Dr Heinz Pitsch and Dr Sivaram Ambikasaran for valuable discussions on this work.

Funding

The first author gratefully acknowledges support from the New Faculty Initiation Grant [project number MEE/15–16/845/NFIG] offered by the Indian Institute of Technology Madras.

Supplemental data

The supplementary materials for this article can be accessed at <https://krithikasivaram.github.io>.

ORCID

Krithika Narayanaswamy  <http://orcid.org/0000-0003-2149-8007>

Perrine Pepiot  <http://orcid.org/0000-0001-9870-2809>

References

- [1] P. Dagaut, M. Reuillon, J.-C. Boettner, and M. Cathonnet, *Kerosene combustion at pressures up to 40 atm: experimental study and detailed chemical kinetic modeling*, Symp. (Int.) Combust. 25 (1) (1994), pp. 919–926.
- [2] R.P. Lindstedt and L.Q. Maurice, *Detailed chemical-kinetic model for aviation fuels*, J. Prop. Power. 16 (2000), pp. 187–195.
- [3] P. Dagaut, *On the kinetics of hydrocarbons oxidation from natural gas to kerosene and diesel fuel*, Phys. Chem. Chem. Phys. 4 (2002), pp. 2079–2094.
- [4] A. Violi, S. Yan, E. G. Eddings, A. F. Sarofim, S. Granata, T. Faravelli, and E. Ranzi, *Experimental formulation and kinetic model for JP-8 surrogate mixtures*, Combust. Sci. Technol. 174 (2002), pp. 399–417.
- [5] C. J. Montgomery, S. Cannon, M. Mawid, and B. Sekar, *Reduced chemical kinetic mechanisms for JP-8 combustion*, 40th AIAA Aerospace Sciences Meeting and Exhibit, Reno, NV, AIAA 2002-0336.
- [6] A. Agosta, N.P. Cernansky, D.L. Miller, T. Faravelli, and E. Ranzi, *Reference components of jet fuels: kinetic modeling and experimental results*, Exp. Thermal Fluid Sci. 28 (2004), pp. 701–708.
- [7] C. Doute, J.-L. Delfau, R. Akrich, and C. Vovelle, *Chemical structure of atmospheric pressure premixed n-decane and kerosene flames*, Combust. Sci. Technol. 105 (1995), pp. 327–344.
- [8] C. Guéret, *Elaboration d'un modèle cinétique pour l'oxydation du kérosène et d'hydrocarbures représentatifs*, Ph.D. thesis, Université d'Orléans (1989).
- [9] M. Colket, T. Edwards, S. Williams, N.P. Cernansky, D.L. Miller, F. Egofoopoulos, P. Lindstedt, K. Seshadri, F.L. Dryer, C.K. Law, D. Friend, D.B. Lenhart, H. Pitsch, A. Sarofim, M. Smooke, and W. Tsang, *Development of an experimental database and kinetic models for surrogate jet fuels*, in: 45th AIAA Aerospace Sciences Meeting and Exhibit, Reno, NV, 2007, pp. 2007–770.
- [10] E. Ranzi, *A wide-range kinetic modeling study of oxidation and combustion of transportation fuels and surrogate mixtures*, Energy Fuels 20 (2006), pp. 1024–1032.
- [11] P. Pepiot-Desjardins, *Automatic strategies for chemical mechanism reduction*, Ph.D. thesis, Stanford University, Department of Mechanical Engineering, 2008.

- [12] S. Dooley, S.H. Won, M. Chaos, J. Heyne, Y. Ju, F.L. Dryer, K. Kumar, C.J. Sung, H. Wang, M.A. Oehlschlaeger, R.J. Santoro, and T.A. Litzinger, *A jet fuel surrogate formulated by real fuel properties*, Combust. Flame 157 (2010), pp. 2333–2339.
- [13] S. Dooley, S.H. Won, J. Heyne, T.I. Farouk, Y. Ju, F.L. Dryer, K. Kumar, X. Hui, C.J. Sung, H. Wang, M.A. Oehlschlaeger, V. Iyer, S. Iyer, T.A. Litzinger, R.J. Santoro, T. Malewicki, and K. Brezinsky, *The experimental evaluation of a methodology for surrogate fuel formulation to emulate gas phase combustion kinetic phenomena*, Combust. Flame 159 (2012), pp. 1444–1466.
- [14] S. Dooley, S.H. Won, J. Heyne, T.I. Farouk, Y. Ju, F.L. Dryer, K. Kumar, X. Hui, C.-J. Sung, H. Wang, M.A. Oehlschlaeger, V. Iyer, S. Iyer, T.A. Litzinger, R.J. Santoro, T. Malewicki, and K. Brezinsky, *The experimental evaluation of a methodology for surrogate fuel formulation to emulate gas phase combustion kinetic phenomena*, Combust. Flame 159 (2012), pp. 1444–1466.
- [15] S.H. Won, S. Dooley, P.S. Veloo, H. Wang, M.A. Oehlschlaeger, F.L. Dryer, and Y. Ju, *The combustion properties of 2, 6, 10-trimethyl dodecane and a chemical functional group analysis*, Combust. Flame 161 (2014), pp. 826–834.
- [16] J. Yu, Y. Ju, and X. Gou, *Surrogate fuel formulation for oxygenated and hydrocarbon fuels by using the molecular structures and functional groups*, Fuel 166 (2016), pp. 211–218.
- [17] M. Mehl, J.-Y. Chen, W.J. Pitz, S. Sarathy, and C.K. Westbrook, *An approach for formulating surrogates for gasoline with application toward a reduced surrogate mechanism for cfd engine modeling*, Energy Fuels 25 (2011), pp. 5215–5223.
- [18] K. Narayanaswamy, H. Pitsch, and P. Pepiot, *A component library framework for deriving kinetic mechanisms for multi-component fuel surrogates: Application for jet fuel surrogates*, Combust. Flame 165 (2016), pp. 288–309.
- [19] P. Pepiot, R. Malhotra, A.R. Kirby, A.L. Boehman, and H. Pitsch, *Experimental study and structural group analysis for soot reduction tendency of oxygenated fuels*, Combust. Flame 154 (2008), pp. 191–205.
- [20] T. Edwards, *Kerosene fuels for aerospace propulsion-composition and properties*, 38th AIAA/ASME/SAE/ASEE Joint Propulsion Conference & Exhibit, Indianapolis, IN, AIAA 2002-3874.
- [21] T. Edwards, *Liquid fuels and propellants for aerospace propulsion: 1903–2003*, J Propuls. Power 19 (2003), pp. 1089–1107.
- [22] Y. Yang, A.L. Boehman, and R.J. Santoro, *A study of jet fuel sooting tendency using the threshold sooting index (tsi) model*, Combust. Flame 149 (1), (2007) pp. 191–205.
- [23] Defense Energy Support Centre, *Petroleum quality information systems*, Ann. Rep. Available at <http://www.desc.dla.mil/DCM/Files/2004PQISreportsmall.pdf> (2008).
- [24] Fuel user guide – average survey data, Tech. rep., US Army Tank-Automotive RD&E Center, Fuels and Lubricants Team, Warren, MI (2000).
- [25] M. Huber, E. Lemmon, and T. Bruno, *Surrogate mixture models for the thermophysical properties of aviation fuel jet-a*, Energy Fuels 24 (2010), pp. 3565–3571.
- [26] D.R. Olson, N.T. Meckel, and R. Quillian Jr, *Combustion characteristics of compression ignition engine fuel components*, Tech. rep., SAE Technical Paper (1960).
- [27] M.J. Murphy, J.D. Taylor, and R.L. McCormick, *Compendium of experimental cetane number data*, Tech. rep., National Renewable Energy Laboratory (NREL), Golden, CO. (2004).
- [28] A. Agosta, *Development of a chemical surrogate for jp-8 aviation fuel using a pressurized flow reactor*, Master’s thesis, Drexel University (2002).
- [29] P. Ghosh and S.B. Jaffe, *Detailed composition-based model for predicting the cetane number of diesel fuels*, Ind. Engg. Chem. Res. 45 (1) (2006), pp. 346–351.
- [30] H. Wang and M.A. Oehlschlaeger, *Autoignition studies of conventional and fischer-tropsch jet fuels*, Fuel 98 (2012), pp. 249–258.
- [31] X. Hui, K. Kumar, C.-J. Sung, T. Edwards, and D. Gardner, *Experimental studies on the combustion characteristics of alternative jet fuels*, Fuel 98 (2012), pp. 176–182.
- [32] K. Narayanaswamy, G. Blanquart, and H. Pitsch, *A consistent chemical mechanism for the oxidation of substituted aromatic species*, Combust. Flame 157 (10) (2010), pp. 1879–1898.
- [33] K. Narayanaswamy, P. Pepiot, and H. Pitsch, *A chemical mechanism for low to high temperature oxidation of n-dodecane as a component of transportation fuel surrogates*, Combust. Flame 161 (4) (2014), pp. 866–884.

- [34] K. Narayanaswamy, H. Pitsch, and P. Pepiot, *A chemical mechanism for low to high temperature oxidation of methylcyclohexane as a component of transportation fuel surrogates*, *Combust. Flame* 162 (2015), pp. 1193–1213.
- [35] H. Wang, E. Dames, B. Sirjean, D.A. Sheen, R. Tangko, A. Violi, J.Y.W. Lai, F.N. Egolfopoulos, D.F. Davidson, R.K. Hanson, C.T. Bowman, C.K. Law, W. Tsang, N.P. Cernansky, D.L. Miller, and R.P. Lindstedt, *A high-temperature chemical kinetic model of n-alkane (up to n-dodecane), cyclohexane, and methyl-, ethyl-, n-propyl and n-butyl-cyclohexane oxidation at high temperatures*, JetSurF version 2.0, Available at <http://web.stanford.edu/group/haiwanglab/JetSurF/> (September 19 2010).
- [36] S.G. Johnson, The NLOpt nonlinear-optimization package. Available at <http://ab-initio.mit.edu/wiki/index.php/NLOpt>
- [37] H. Pitsch, M. Bollig, *Flamemaster, a computer code for homogeneous and one-dimensional laminar flame calculations*, Institut für Technische Mechanik, RWTH Aachen.
- [38] S.G. Davis, A.B. Mhadeshwar, D.G. Vlachos, H. Wang, *A new approach to response surface development for detailed gas-phase and surface reaction kinetic model optimization*, *Int. J. Chem. Kinetics* 36 (2004), pp. 94–106.